

A new Meckel's cartilage from the Devonian Hangenberg black shale in Morocco and its position in chondrichthyan jaw morphospace (#76196)

1

First revision

Guidance from your Editor

Please submit by **15 Oct 2022** for the benefit of the authors (and your token reward) .



Structure and Criteria

Please read the 'Structure and Criteria' page for general guidance.



Custom checks

Make sure you include the custom checks shown below, in your review.



Raw data check

Review the raw data.



Image check

Check that figures and images have not been inappropriately manipulated.

Privacy reminder: If uploading an annotated PDF, remove identifiable information to remain anonymous.

Files

Download and review all files from the [materials page](#).

- 1 Tracked changes manuscript(s)
- 1 Rebuttal letter(s)
- 7 Figure file(s)
- 1 Table file(s)
- 1 Raw data file(s)

! Custom checks

Field study

- ! Have you checked the authors [field study permits](#)?
- ! Are the field study permits appropriate?




Structure and Criteria

Structure your review

The review form is divided into 5 sections. Please consider these when composing your review:

1. BASIC REPORTING
2. EXPERIMENTAL DESIGN
3. VALIDITY OF THE FINDINGS
4. General comments
5. Confidential notes to the editor

 You can also annotate this PDF and upload it as part of your review

When ready [submit online](#).

Editorial Criteria

Use these criteria points to structure your review. The full detailed editorial criteria is on your [guidance page](#).




BASIC REPORTING

-  Clear, unambiguous, professional English language used throughout.
-  Intro & background to show context. Literature well referenced & relevant.
-  Structure conforms to [Peerj standards](#), discipline norm, or improved for clarity.
-  Figures are relevant, high quality, well labelled & described.
-  Raw data supplied (see [Peerj policy](#)).

EXPERIMENTAL DESIGN

-  Original primary research within [Scope of the journal](#).
-  Research question well defined, relevant & meaningful. It is stated how the research fills an identified knowledge gap.
-  Rigorous investigation performed to a high technical & ethical standard.
-  Methods described with sufficient detail & information to replicate.

VALIDITY OF THE FINDINGS

-  Impact and novelty not assessed. *Meaningful* replication encouraged where rationale & benefit to literature is clearly stated.
-  All underlying data have been provided; they are robust, statistically sound, & controlled.
-  Conclusions are well stated, linked to original research question & limited to supporting results.



The best reviewers use these techniques

Tip

Example

Support criticisms with evidence from the text or from other sources

Smith et al (J of Methodology, 2005, V3, pp 123) have shown that the analysis you use in Lines 241-250 is not the most appropriate for this situation. Please explain why you used this method.

Give specific suggestions on how to improve the manuscript

Your introduction needs more detail. I suggest that you improve the description at lines 57- 86 to provide more justification for your study (specifically, you should expand upon the knowledge gap being filled).

Comment on language and grammar issues

The English language should be improved to ensure that an international audience can clearly understand your text. Some examples where the language could be improved include lines 23, 77, 121, 128 - the current phrasing makes comprehension difficult. I suggest you have a colleague who is proficient in English and familiar with the subject matter review your manuscript, or contact a professional editing service.

Organize by importance of the issues, and number your points

1. Your most important issue
2. The next most important item
3. ...
4. The least important points

Please provide constructive criticism, and avoid personal opinions

I thank you for providing the raw data, however your supplemental files need more descriptive metadata identifiers to be useful to future readers. Although your results are compelling, the data analysis should be improved in the following ways: AA, BB, CC

Comment on strengths (as well as weaknesses) of the manuscript

I commend the authors for their extensive data set, compiled over many years of detailed fieldwork. In addition, the manuscript is clearly written in professional, unambiguous language. If there is a weakness, it is in the statistical analysis (as I have noted above) which should be improved upon before Acceptance.

A new Meckel's cartilage from the Devonian Hangenberg black shale in Morocco and its position in chondrichthyan jaw morphospace

Merle Greif ^{Corresp., 1}, Humberto Ferrón ², Christian Klug ¹

¹ Palaeontological Institute and Museum, University of Zürich, Zürich, Switzerland

² Instituto Cavanilles de Biodiversidad i Biología Evolutiva, Universitat de València, 46980 Paterna, Valencia,, Spain

Corresponding Author: Merle Greif
Email address: merle.greif@pim.uzh.ch

Fossil chondrichthyan remains are mostly known from their teeth, scales or fin spines only, whereas their cartilaginous endoskeletons require exceptional preservational conditions to become fossilized. While most cartilaginous remains of Famennian (Late Devonian) chondrichthyans were found in older layers of the eastern Anti-Atlas, such fossils were unknown from the Hangenberg black shale (HBS) and only a few chondrichthyan teeth had been found therein previously. Here, we describe a Meckel's cartilage from the Hangenberg black shale in Morocco, which is the first fossil cartilage from these strata. Since no teeth or other skeletal elements have been found in articulation, we used elliptical Fourier (EFA), principal component (PCA), and hierarchical cluster (HCA) analyses to morphologically compare it with 41 chondrichthyan taxa of different size and age and to evaluate its possible systematic affiliation. PCA and HCA position the new specimen closest to some acanthodian and elasmobranch jaws. Accordingly, a holocephalan origin was excluded. The jaw shape as well as the presence of a polygonal pattern, typical for tessellated calcified cartilage, suggest a ctenacanth origin and we assigned the new HBS Meckel's cartilage to the order Ctenacanthiformes with reservations.

1 **A new Meckel's cartilage from the Devonian**
2 **Hangenberg black shale in Morocco and its**
3 **position in chondrichthyan jaw morphospace**

4
5 Merle Greif¹, Humberto G. Ferrón², Christian Klug¹

6
7 ¹ Palaeontological Institute and Museum, University Zurich, 8006, Zurich, Switzerland.

8 ² Instituto Cavanilles de Biodiversidad i Biología Evolutiva, Universitat de València, C/
9 Catedrático José Beltrán Martínez, 2, 46980 Paterna, Valencia, Spain; School of Earth
10 Sciences, University of Bristol, Life Sciences Building, Bristol BS8 1TH, UK.

11
12 Corresponding Author:

13 Merle Greif¹
14 University Zurich, Karl-Schmid-Strasse 4, 8006, Zurich, Switzerland.
15 Email address: merle.greif@pim.uzh.ch

16
17 **Abstract**

18
19 Fossil chondrichthyan remains are mostly known from their teeth, scales or fin spines
20 only, whereas their cartilaginous endoskeletons require exceptional preservational
21 conditions to become fossilized. While most cartilaginous remains of Famennian (Late
22 Devonian) chondrichthyans were found in older layers of the eastern Anti-Atlas, such
23 fossils were unknown from the Hangenberg black shale (HBS) and only a few
24 chondrichthyan teeth had been found therein previously. Here, we describe a Meckel's
25 cartilage from the Hangenberg black shale in Morocco, which is the first fossil cartilage
26 from these strata. Since no teeth or other skeletal elements have been found in
27 articulation, we used elliptical Fourier (EFA), principal component (PCA), and
28 hierarchical cluster (HCA) analyses to morphologically compare it with 41
29 chondrichthyan taxa of different size and age and to evaluate its possible systematic
30 affiliation. PCA and HCA position the new specimen closest to some acanthodian and

31 elasmobranch jaws. Accordingly, a holocephalan origin was excluded. The jaw shape
32 as well as the presence of a polygonal pattern, typical for tessellated calcified cartilage,
33 suggest a ctenacanth origin and we assigned the new HBS Meckel's cartilage to the
34 order Ctenacanthiformes with reservations.

35

36 **Introduction**

37

38 Fossil chondrichthyans (sharks, rays and chimaeroids) are mainly known from the
39 Devonian onward (Brazeau & Friedman 2015). Exceptional, putative chondrichthyan, as
40 well as acanthodian finds date back to the Silurian (Burrow & Rudkin 2014; Andreev et
41 al. 2016). Only teeth, scales and fin spines of chondrichthyans (whole group, including
42 acanthodians) are strongly mineralized while chondrichthyan endoskeletons are
43 predominantly made of unmineralized cartilage that is only rarely preserved (Seidel et
44 al. 2020).

45 Despite the difficulties of preservation, chondrichthyan skeletons are frequently found in
46 the middle and late Famennian strata in the Tafilalt and Maïder regions of southern
47 Morocco and constitute important contributions to the understanding of early vertebrates
48 (Ginter et al. 2002; Derycke et al. 2008; Frey et al. 2018; Frey et al. 2020). However, in
49 the late Famennian Hangenberg black shale layers of Morocco, nearly no vertebrate
50 remains have been collected or described so far. The only known contributions to the
51 vertebrate fossil record that are known from these strata are a few chondrichthyan
52 teeth, which are not described but only mentioned in the literature (Klug et al 2016; Frey
53 et al. 2018) as well as some chondrichthyan ichnofossils from layers just above the
54 Hangenberg black shale (basal Hangenberg Sandstone; Klug et al 2021). Here, we

55 describe a lower jaw found in the Anti-Atlas that represents the first reported
56 cartilaginous remain from the Moroccan Hangenberg black shale.
57 Outcrops of sediments that were laid down in the time around the end-Devonian
58 Hangenberg crisis can be found at many localities of the Tafilalt and Maïder regions of
59 the Anti-Atlas (Kaiser et al. 2011, 2015; Klug et al. 2021). The Hangenberg crisis was a
60 global mass extinction event at the Devonian/ Carboniferous boundary (Caplan & Bustin
61 1999; Kaiser et al. 2011), which reflects one of the six largest mass extinction events in
62 earth's history. The Hangenberg crisis followed the Kellwasser event at the Frasnian/
63 Famennian boundary and affected vertebrate groups to an extent that is comparable to
64 the Big Five mass extinctions (McGhee 1996; McGhee et al 2012, 2013). Therefore, it is
65 seen as a bottleneck in vertebrate evolution and the recovery of formerly diverse
66 vertebrate groups (such as some agnathans, sarcopterygians and placoderms) after
67 the event was minimal (Sallan and Coates 2010; Frey et al. 2018). Indeed, the
68 Hangenberg crisis was more severe than formerly thought and caused a larger diversity
69 **loss** on genus level than the Kellwasser event (Sallan & Coates 2010). The Hangenberg
70 black shale marks the main extinction phase of the event and was laid down during a
71 supposed global transgression linked with widespread anoxia, likely caused by
72 eutrophication that led to global extinctions of numerous **invertebrate** groups (Algeo &
73 Scheckler 1998; Sallan & Coates 2010; Kaiser et al 2011, 2015). While **invertebrate**
74 remains are quite common in the Hangenberg black shale (Schmidt, 1924; Marynowski
75 et al. 2012; Klug et al. 2016; Zhang et al. 2019), it lacks vertebrate remains, which
76 makes the new Meckel's cartilage a particularly important fossil.

77 The cartilaginous endoskeletons of chondrichthyans are covered by a thin layer of
78 calcified cartilage (Kemp & Westrin 1979; Dean & Summers 2006, Seidel et al. 2016,
79 2020; Maisey et al. 2020). This thin layer typically shows a distinct polygonal pattern,
80 which is caused by the presence of tesserae, namely the tessellated calcified cartilage
81 (Seide et al. 2016, 2020, 2021; Maisey et al. 2020). Such cartilage is characteristic for
82 **modern** as well as Devonian crown chondrichthyans (elasmobranchs and
83 holocephalans, Long et al. 2015; Maisey 2020) while these polygonal structures tend to
84 be less distinct in acanthodians (stem **chondrichthyans**), where only subtessellated
85 calcified cartilage or globular calcified cartilage is reported (Dean & Summers 2006;
86 Brazeau & Friedman 2014; Brazeau 2020; Maisey et al. 2020). Globular calcified
87 cartilage builds the inner layer of tessellated calcified cartilage and can build the entire
88 hard tissue. If globular calcified cartilage is present on the surface a granular pattern is
89 to **expect** (Burrow et al. 2015; Maisey et al. 2020). Subtessellated calcified cartilage
90 shows fissures along the **surface** which result in an unorganized pattern. Tessellated
91 calcified cartilage with an outer prismatic layer, in contrast, is well organized and a
92 polygonal pattern is distinct (Maisey et al. 2020; Seidel et al. 2020).

93 Among the cartilaginous remains, jaws are one of the most relevant anatomical
94 structures from an evolutionary perspective. The evolution of jaws, the Meckel's
95 cartilage, is seen as a key innovation of gnathostomes enabling the first gnathostomes
96 to broaden their range of feeding strategies and prey upon a much greater diversity of
97 animals (DeLaurier & Gerhart, 2018; Deakin et al. 2022). These innovations contributed
98 greatly to the radiation of gnathostomes and possibly to the decline of agnathans
99 (Brazeau & Friedman 2015; Hill et al. 2018). Nevertheless, only very few quantitative

100 studies about jaw shapes have been published. For example, Hill et al. (2018)
101 quantified jaw shape in **modern** and in Palaeozoic **fishes** and demonstrated that jaw
102 shape has a greater disparity in modern fish clades than during the early gnathostome
103 radiation (Silurian and Devonian). This is mostly caused by the great morphological
104 disparity among **modern** actinopterygians (Hill et al. 2018). Deakin et al. (2022) also
105 mentioned an increasing disparity in jaw shape with ongoing evolution but the functional
106 disparity of early vertebrate jaws to be highest very early in jaw evolution and optimized
107 for a predatory function. Anderson et al. 2011 also deals with jaw disparity and the
108 influence of environmental changes such as the Kellwasser event, which does not seem
109 to affect jaw disparity very much.

110 The phylogenetic relations within the chondrichthyan total group are still a widely
111 discussed topic (Hanke & Wilson 2006; Brazeau 2009; Davis et al. 2012; Burrow &
112 Rudkin 2014; Brazeau & Friedman 2015; Brazeau & de Winter 2015; Giles et al 2015;
113 Qiao et al. 2016) and acanthodians were just recently recognized as stem
114 chondrichthyans (Zhu et al. 2013; Coates et al. 2017; Rücklin et al. 2021). Members of
115 this group show characteristics of both principal **lineages** of living gnathostomes
116 (chondrichthyans and osteichthyans), are covered with scales and are often referred to
117 as “spiny sharks” because of the spines in front of their dorsal, anal and paired fins as
118 evident in most taxa of this group (Miles 1970, 1973; Burrow & Rudkin 2014; Qiao et al.
119 2016). The relationship between jaw shape and phylogeny remains an elusive question
120 since ecological factors likely influence jaw shape to a great degree as well.
121 Our main aim in this article is, 1) to give a detailed description of this novel find and 2) to
122 determine its possible systematic affiliation. For the latter, we used geometric

123 morphometrics since the Meckel's cartilage was found ~~solitarily~~ with no further skeletal
124 parts, teeth or scales associated and is therefore hard to assign to a specific taxon. We
125 applied elliptical Fourier (EFA), principal component (PCA) and hierarchical cluster
126 analyses (HCA) to the new small Meckel's cartilage and 41 more chondrichthyan and
127 acanthodian lower jaws. By this action, a morphospace is created which is informative
128 about the relationship between lower jaw shape and phylogeny.

129

130 **Materials & Methods**

131

132 The specimen PIMUZ A/I 5139 (Fig.1) was found in the Moroccan Anti-Atlas at the
133 locality Madene El Mrakib (N30.73093°, W4.70749°). Permit for fossil collection and
134 export were given by the Ministère de l'Energie, des Mines, de l'Eau et de
135 l'Environnement, Rabat, Morocco. The specimen is stored at the Palaeontological
136 Institute and Museum of Zurich (Switzerland). It was largely exposed, but covered parts
137 were carefully prepared using a thin steel-needle. Photos of the specimen showing its
138 shape, proportions and preservation (Fig. 1) were taken using a Nikon D2X. Colour and
139 contrast were slightly adjusted in Adobe Photoshop (Adobe Inc. 2019). To show the
140 structure of the fossil's surface in more detail, close-ups were taken with a Leica MZ16
141 F microscope (Fig. 1C, D, E) and gently adjusted in colour and contrast as well.

142

143 **Morphometrics**

144 Morphometric techniques together with multivariate and cluster analysis are standard
145 methods to quantify morphology and evaluate groupings or affinities among taxa
146 (Kaesler & Waters 1972; Younker & Ehrlich 1977; Ferrario et al. 1999; Daegling &

147 Jungers 2000). Here, we use morphometric analyses to compare the new isolated
148 Meckel's cartilage to shapes of other lower jaws with known systematic affiliation and
149 find the most similar shape, or group of shapes, to help determine the new Meckel's
150 cartilage origin at least approximately. To carry out the analyses, outlines of 41 lower
151 jaws representing the main stem and crown chondrichthyan orders were drawn based
152 on photographs and illustrations from the literature (App. 1) using the vector-based
153 software Affinity Designer (Affinity 2019). Sampling is constrained by the limited number
154 of well-preserved fossils of Meckel's cartilages. The jaw shapes used in the analysis
155 were chosen based on the quality of preservation and completeness of the Meckel's
156 cartilage as could be seen in the publications. The sampled jaws belong to taxa from
157 different periods and localities and cover a wide range of sizes (App. 2). This broad
158 sampling range (regarding time, locality and size) was used to find general differences
159 in shape between the different groups. All Meckel's cartilage outlines were digitized in
160 TPS software (Rohlf, 2015). Elliptic Fourier Analysis (EFA) was then performed in the
161 Momocs package (Bonhomme et al., 2014) in R (R Development Core Team, 2020) to
162 statistically compare all sampled lower jaw shapes. A total number of 25 harmonics
163 were considered, which gather nearly 99% of the cumulative harmonic power (seen as
164 a measure of shape information) and reconstructs actual morphologies with high
165 accuracy. We obtained a virtual morphospace by performing a principal component
166 analysis (PCA, Fig. 2) on the preordination data to plot the main shape variations. To
167 quantify the morphological similarity amongst the studied jaws, a Hierarchical Cluster
168 Analysis (HCA) using the R package 'dendextend' (Galili et al. 2019) was conducted.
169 Phylogenetic signal was assessed using the lambda and K statistic with 1,000 random

170 permutation in the R package 'phytools' (Revell 2012). Additionally, a Mantel test,
171 correlating phenetic (morphological) and phylogenetic distances was performed in order
172 to assess the degree of morphological convergence in our sample. These metrics are
173 expected to show greater decoupling and, consequently, lower correlation where
174 homoplasy occurs. We repeated the tests in a set of 1000 phylogenetic trees that
175 accounted for phylogenetic and stratigraphic uncertainty. The tree topology is based on
176 Klug et al. (ongoing research). Polytomies were randomly resolved 1000 times and
177 each resulting tree was calibrated by randomizing the tip age of every species within the
178 chronostratigraphic unit, at age or subperiod rank, where their first appearance occurs,
179 using the R package 'paleotree'.

180

181

182 **Results**

183

184 **Systematic Palaeontology**

185 Class Chondrichthyes Huxley, 1880

186 Subclass ? Elasmobranchii Bonaparte, 1838

187 Order ? Ctenacanthiformes Glikman, 1964

188

189 The Meckel's cartilage with a total length of 18 mm and a height of up to 6 mm is nearly
190 complete and preserved in lateral view (Fig. 1A). The posterior part is somewhat
191 incomplete in the main plate and entirely missing in the counterpart (Fig. 1A, B, D).
192 While most of the specimen is visibly different from the sediment due to its internal
193 structure and colour, in the posterior part the Meckel's cartilage limits are less clear and

194 the exact borders between fossil and sediment are difficult to determine. The specimen
195 shows a bright grey to white colour and most of it is somewhat brighter than the
196 sediment. In the main fossil plate and in the counterpart, a distinctive polygonal pattern
197 of the calcified cartilage is visible mainly in the posterior part (Fig. 1E_{1,2}) while in the
198 middle to anterior part, the specimen is mineralized in a bright colour. The tessellation is
199 not as geometric as in some modern species (Seidel et al. 2020,2021) but the polygons
200 are distinct. In some areas, the borders of the polygonal tesserae are clearly
201 distinguishable by white outlines that most likely represent the intertesseral fibres
202 (Seidel et al. 2016). Even though the tesserae borders are distinct, the corners, as well
203 as the borders in general are rounded and less distinct. Despite the blurriness, the
204 pattern is very similar to the one that can be seen in the crown chondrichthyan
205 *Tristychius arcuatus* (Brazeau & Friedman 2014, fig. 5C, D).

206 The ventral edge of the Meckel's cartilage is gently convexly curved. The ventral ridge is
207 discernible in spite of the **compaction**, especially in the middle to posterior part. It follows
208 the shape of the outline of the jaw until about 2.5 mm distance from the posterior end
209 when it bends upwards (Fig. 1A). The Meckel's cartilage becomes higher from
210 posteriorly until just before the articulation. It displays one bulge at the thickened
211 anterior end, which is about 4 mm long and might represent the symphysis. This bulge
212 is followed by a shallow depression, which is 3.5 mm long and a shallow bulge of about
213 2.5 mm length. The preservation is insufficient to identify muscle attachments with
214 confidence. We assume that the anterior 9 mm was the tooth-bearing part (dental
215 sulcus) because the concave upper edge anterior to the articulation ends there and it
216 appears like the dorsal side broadens from this point anteriorly. The next depression

217 extends over 7.5 mm and ends at the articulation. Although the specimen is flattened,
218 the retroarticular flange (cf. Long et al. 2015) at the posterior end is still preserved as a
219 knob. The articulation is positioned dorsally in the posterior end of the jaw but
220 unfortunately the preservation does not allow to determine the exact shape of the
221 articulation and it seems incomplete.

222

223 **Morphometric Analyses**

224 The PCA shows clear separation between the jaws of the two chondrichthyan clades
225 Elasmobranchii and Holocephalii (Fig. 2). PC 1 (59% of variance) is mostly related to
226 changes in jaw thickness with decreasing thickness from negative to positive scores.
227 PC 2 (13% of variance) mainly reflects changes of the jaw curvature (from strongly
228 convex to slightly concave), with a decrease in curvature from negative to positive
229 scores (Fig. 2). PC 3 (6% of variance) mostly describe changes in the curvature of the
230 anterior end of the jaw as well as changes of the roundness of the posteroventral edge
231 of the jaw (Fig. 2). Holocephalan jaws occupy high PC1 scores of about 0.05 to 0.17
232 and positive PC2 scores and show relatively slender and only slightly curved
233 morphologies. Elasmobranch jaws occupy a wider score range with PC1 scores
234 between -0.8 to 0.08 and PC2 scores between 0.07 and 0.10 (Fig. 2). Most of them plot
235 in the centre of the morphospace between PC1 scores of about -0.5 and 0.01 and PC2
236 scores around 0.0. Elasmobranch jaws show a greater shape variation than
237 holocephalan jaws, from thick and bulky to relatively slender. Acanthodian jaws occupy
238 PC1 scores from -0.11 to 0.10 and PC2 scores of -0.12 to 0.05 (Fig. 2) and overlap to a
239 large extent with elasmobranch and holocephalan jaws. Acanthodian jaw shapes vary

240 from bulky and curved to slender and straight. The new specimen plots at -0.01/0.025
241 (PC1/PC2), which is close to the other sampled acanthodians and some
242 elasmobranchs. The new specimen plots **closest to the acanthodian taxa** *Ischnacanthus*
243 *sp.* and *Latviacanthus ventspilsensis*. Furthermore, some ctenacanth plots very close:
244 *Dracopristis hoffmanorum*, *Ctenacanthus sp.* *Heslerodus divergens*, as well as another
245 elasmobranch of the order Synechodontiformes: *Palidiplospinax occultidens* (Fig. 2).
246 In the dendrogram derived from the HCA, the new Hangenberg black shale Meckel's
247 cartilage plots closest to the acanthodian *Latviacanthus ventspilsensis*. The
248 acanthodian *Ischnacanthus sp.* and the elasmobranch of *Heslerodus divergens*
249 constitute **sequential outgroups** to those two (Fig. 3). Overall, there is not a clear
250 grouping among the three classes (Fig. 3). However, at a lower clustering rank, a
251 separation between holocephalans and elasmobranchs is supported while acanthodians
252 plot together with either elasmobranchs or holocephalans (Fig. 3). We find a significant
253 phylogenetic signal as measured by the metrics K (equal to 0.501 ± 0.071 ; p -value =
254 0.004 ± 0.004) and lambda (equal to 0.995 ± 0.123 ; p -value = 0.0001 ± 0.0001 ; Fig. 4),
255 but no significant correlation in between phenetic and phylogenetic distances in the
256 Mantel tests (R statistic = -0.045 ± 0.009 ; p -value = 0.632 ± 0.032 , all data expressed in
257 mean \pm standard deviation, Fig. 5).

258

259 Discussion

260 Our methodological framework based on EFA, PCA and HCA allows for discriminating
261 holocephalans from elasmobranchs as well as some clades of lower systematic rank,
262 but discrimination of acanthodians as a whole from holocephalans and elasmobranchs
263 is not evident (Figs. 2, 3). We detect a strong phylogenetic signal in our dataset (Fig. 4),

264 altogether suggesting that outline jaw shape by itself can be, to some extent,
265 informative for systematic placement of disarticulated remains and add support to other
266 evidence. However, it has to be kept in mind, that our morphometric analysis considers
267 two-dimensional outline shape and, potentially, some relevant anatomical information to
268 discriminate among other groups might not be captured. Further, the lack of correlation
269 in Mantel tests (Fig. 5) entail the presence of homoplasy, which might hinder the
270 interpretations of phylogenetic affinity from general morphology. Similarities in jaw
271 shape can also result from adaptation. Jaw shape can, for example, be an adaption to a
272 certain lifestyle as in durophagous sharks (Herbert & Motta 2018) or in general be
273 connected to diet in combination with water depth (Motta & Huber 2012). Small
274 variations in shape could also occur due to fossilisation, preparation and errors in
275 redrawing the different outlines, but we do not expect this to have a major effect in our
276 results as preliminary studies have supported that biological signal is still well preserved
277 when minor taphonomical alterations exist (Angielczyk & Sheets 2007).

278 The inclusion of the new Hangenberg black shale jaw in the analysis revealed that it is
279 most similar in shape to lower jaws of certain acanthodian (i.e., *Ischnacanthus sp.* and
280 *Latviacanthus ventspilsensis*) as well as elasmobranchs (the ctenacanth *Dracopristis*
281 *hoffmanorum*, *Ctenacanthus sp.*, and *Heslerodus divergens*; and the synechodontiform
282 *Palidiplospinax occultidens*) (Figs. 2, 3). A holocephalan affinity is unlikely as all
283 considered taxa from this group fall in a separate area of the morphospace. The
284 Hangenberg black shale jaw sits slightly closer to acanthodian jaw shapes than to
285 elasmobranch jaw shapes but whether it is of acanthodian or of elasmobranch origin is

286 difficult to ascertain solely from those analyses and further information is needed to
287 determine its possible origin.

288 Besides the HBS Meckel's cartilage, the only vertebrate fossils known from the
289 Hangenberg black shale are some poorly preserved chondrichthyan teeth (Klug et al.
290 2016), which are not determined but could be of symmoriiform origin (? *Stethacanthus*,
291 Coates & Sequeira 2001, fig. 5 F-I). However, given the analyses a holocephalan origin
292 seems unlikely. The exclusion of a holocephalan origin is further supported by the
293 absence of a terminally positioned articulation which is typical for holocephalans
294 (Coates et al. 2017, character matrix). Due to incomplete preservation of the articulation,
295 it cannot be compared in detail to other chondrichthyan lower jaws.

296 Among the few characters present in the new HBS Meckel's cartilage, some can help to
297 further distinguish its most probable affinity. Thus, the jaw of the ctenacanth *Heslerodus*
298 *divergens* (Hodnett et al. 2021) seems to share some features not directly captured by
299 outline analysis, which are less distinct in both acanthodian jaws that plot close to the
300 HBS jaw. The jaw of *Heslerodus divergens* has a relatively thin anterior to middle part
301 comparable to the first 9 mm of the new jaw that we described as the probable tooth
302 bearing part. Following this, in both jaw shapes, a ridge is present leading to a second
303 depression that ends in the articulation. In the jaw of *Heslerodus divergens* this shape is
304 more distinct than in the HBS jaw while both acanthodian jaws are dorsally straighter
305 shaped (Fig. 6). Additionally, Hodnett et al. (2021) describes "a well-developed ventral
306 ridge on the lateral margin of the Meckel's cartilage, that extends over two thirds the
307 length of the jaw", as a synapomorphy of ctenacanth. A ventral ridge is one of the few
308 features of the new Hangenberg black shale jaw, that is well recognizable (Fig. 1).

309 *Ischnacnathus sp.* shows a ventral ridge as well but when comparing the HBS jaw
310 ventral ridge to the other two, the one of *Heslerodus divergens* is a lot more similar
311 (Fig.6).

312 In addition, a distinct polygonal structure is visible on the surface of the jaw (Fig. 1C).
313 This pattern is characteristic for tessellated calcified cartilage, which is widely accepted
314 as a synapomorphy of modern and extinct crown chondrichthyans (Brazeau & Friedman
315 2014; Long, et al. 2015; Seidel et al. 2016, 2021; Maisey et al. 2020). Tessellated
316 calcified cartilage is made of an inner layer of globular calcified cartilage and an outer
317 layer of prismatic calcified cartilage (Maisey et al 2020). Only the outer prismatic layer
318 shows the typical polygonal pattern while the globular calcified cartilage shows a
319 granular surface (see for example the acanthodian *Climatius reticulatus* in Burrow et al.
320 2015, fig. 1, I).

321 Fossils of the acanthodian group (stem chondrichthyans) mostly do not show a
322 polygonal pattern, since no prismatic outer layer is present but only globular calcified
323 cartilage (Maisey et al. 2020). However, Maisey et al. (2020) describes the presence of
324 subtessellated calcified cartilage in some acanthodians, while actual tessellated
325 calcified cartilage (showing the outer prismatic layer) is apparently absent (Brazeau &
326 Friedman 2014). Acanthodians like *Climatius* (Burrow et al. 2015), *Ischnacanthus*
327 (Burrow et al. 2018) or *Cheiracanthus* (den Blaauwen 2019) are mentioned to show this
328 subtessellated calcified cartilage. When looking at *Climatius*, it appears granular and no
329 actual polygons are visible on the surface as mentioned above (Burrow et al. 2015, fig.
330 1, I). In *Ischnacanthus* (Burrow et al. 2018), a subtessellated calcified cartilage is
331 described using histology; we cannot compare the HBS specimen to that. In

332 *Cheiracanthus* (den Blaauwen 2019), the surface appears “*globular or randomly*
333 *tessellated*”. To sum this up, acanthodian fossils, or stem chondrichthyans, show a
334 rather globular or irregular pattern (Burrow et al 2015 fig. 1, I; Long et al. 2015, fig. 9, A),
335 which differs a lot from the regular polygonal pattern in crown chondrichthyans.
336 A polygonal pattern is evident in the new specimen but the borders of the single
337 tesserae are slightly blurred taphonomically, which might have been caused by
338 dissolution of the unmineralized collagen between the tiles (intertesseral fibre; Seidel et
339 al 2016). However, the pattern is distinct and regular, making an elasmobranch origin
340 more likely than an acanthodian origin. In fact, it is as regular as the polygonal pattern in
341 the crown chondrichthyan *Tristychius arcuatus* (Brazeau & Friedman 2014).
342 Based on the results from morphometric analyses and the presence of both a ventral
343 ridge on the lateral margin and tessellated calcified cartilage with a regular polygonal
344 pattern, we assign the new Meckel’s cartilage to the order Ctenacanthiformes with some
345 reservations (Fig. 7). To some degree, this classification remains tentative and a bigger
346 sample size could help to test the hypothesis. Further fossil finds as well as a better
347 understanding of the early development of tessellated calcified cartilage in early fishes
348 could help to classify the new jaw in more detail. However, this study presents an
349 important fossil find, filling a gap in the fossil record and provides crucial information
350 about the difficulties of determining the systematic affiliation of isolated cartilaginous
351 fossil remains.

352

353 **Conclusions**

354 The newly described Meckel’s cartilage is the first known fossil cartilage remain from
355 the Hangenberg black shale from the Moroccan Anti-Atlas. It is 18 mm in length,
356 ventrally convexly curved and shows a biconcave dorsal edge. PCA and HCA reveal a
357 strong similarity in shape with certain acanthodians and elasmobranchs and a

358 phylogenetic signal is detected in our dataset. We **conclude**, that jaw shape can be
359 informative about the systematic placement of disarticulated skeletal elements but
360 further information is needed since **homoplasy is suggested**. The structure of the
361 tessellated calcified cartilage was used as a character for classification. It shows a
362 distinct polygonal pattern which is characteristic for crown chondrichthyans.
363 Furthermore, its general shape as well as the shape of the ventral ridge were compared
364 to two of the jaws that were classified as the most similar by PCA and HCA analyses.
365 This comparison suggests a ctenacanth affiliation. **Considering all** mentioned
366 evidences, we assigned the new lower jaw to the order Ctenacanthiformes, tentatively.
367

368 **Acknowledgements**

369 We thank the Ministère de l'Énergie, des Mines, de l'Eau et de l'Environnement
370 (Direction du Développement Minier, Division du Patrimoine, Rabat, Morocco) for
371 providing working and sample export permits. At an earlier stage, Louis Dudit (Zürich)
372 helped with the Fourier analysis. We showed photos of the Meckel's cartilage to Carole
373 Burrow (Queensland) and Jake Leyhr (Uppsala) and discussed its affiliation. We greatly
374 appreciate their suggestions regarding both the jaw and the teeth from the HBS. We
375 thank the reviewers for XX.

376

377 **References**

- 378 Adobe Inc. 2019: *Adobe Photoshop*, Available at:
379 <https://www.adobe.com/products/photoshop.html>
380
- 381 Affinity 2019: *Affinity Designer*, Available at <https://affinity.serif.com/en-us/designer/>
382
- 383 Algeo, T. J. and Scheckler, S. E. 1998: Terrestrial-marine teleconnections in the Devonian: links
384 between the evolution of land plants, weathering processes, and marine anoxic events.
385 *Philosophical Transactions of the Royal Society London B*353, 113–130.
- 386 Anderson, P. S. L.; Friedman, M.; Brazeau, M.; Rayfield, E. J. 2011: Initial radiation of jaws
387 demonstrated stability despite faunal and environmental change. *Nature* 476, 206-209.
- 388 Andreev, P., Coates, M. I., Karatajūtė-Talimaa, V., Shelton, R. M., Cooper, P. R., Wang, N. Z.,
389 & Sansom, I. J. 2016: The systematics of the Mongolepidida (Chondrichthyes) and the
390 Ordovician origins of the clade. *PeerJ*, 4, e1850.
- 391 Angielczyk, K. D. and Sheets, H. D. 2007: Investigation of simulated tectonic deformation in
392 fossils using geometric morphometrics. *Paleobiology* 33, 125–148.
- 393 Bapst, D. W. 2012: "paleotree: an R package for paleontological and phylogenetic analyses of
394 evolution." *Methods in Ecology and Evolution* 3.5, 803-807.
- 395 Bonhomme, V.; Picq, S.; Gaucherel, C.; Claude, J. 2014: Momocs: outline analysis using R.
396 *Journal of Statistical Software* 56:1–24.
- 397 Brazeau, M. D. 2009: The braincase and jaws of a Devonian 'acanthodian' and modern
398 gnathostome origins. *Nature* 457 (7227), 305–308.

- 399 Brazeau, M. D. 2012: A revision of the anatomy of the Early Devonian jawed vertebrate
400 *Ptomacanthus anglicus* Miles. *Palaeontology* 55 (2), 355–367.
- 401 Brazeau, M. D.; Friedman, M. 2014: The characters of Palaeozoic jawed vertebrates. *Zoological*
402 *Journal of the Linnean Society* 170 (4), 779–821.
- 403 Brazeau, M. D.; Giles, S.; Dearden, R. P.; Jerve, A.; Ariunchimeg, Y. A.; Zorig, E. et al. 2020:
404 Endochondral bone in an Early Devonian 'placoderm' from Mongolia. *Nature Ecology and*
405 *Evolution* 4 (11), 1477–1484.
- 406 Brazeau, M. D. & de Winter, V. 2015: The hyoid arch and braincase anatomy of *Acanthodes*
407 support chondrichthyan affinity of 'acanthodians'. *Proceedings. Biological sciences* 282 (1821),
408 20152210.
- 409 Brazeau, M. D. & Friedman, M. 2015: The origin and early phylogenetic history of jawed
410 vertebrates. *Nature* 520 (7548), 490–497.
- 411 Burrow, C. J.; Blaauwen, J. den; Newman, M. 2020: A redescription of the three longest-known
412 species of the acanthodian *Cheiracanthus* from the Middle Devonian of Scotland.
413 *Palaeontologia Electronica* 23(1): a15.
- 414 Burrow, C. J.; Davidson, R. G.; Den Blaauwen, J. L.; Newman, M. J. 2015: Revision of *Climatius*
415 *reticulatus* Agassiz, 1844 (Acanthodii, Climauidae), from the Lower Devonian of Scotland, based
416 on new histological and morphological data. *Journal of Vertebrate Paleontology* 35 (3),
417 e913421.
- 418 Burrow, C. J.; Newman, M.; Blaauwen, J. den; Jones R.; Davidson, R. G. 2018: The Early
419 Devonian ischnacanthiform acanthodian *Ischnacanthus gracilis* (Egerton, 1861) from the
420 Midland Valley of Scotland. *Acta geologica Polonica* 68 (3), 335–362.
- 421 Burrow, C. J. & Rudkin, D. 2014: Oldest Near-Complete Acanthodian: The First Vertebrate from
422 the Silurian Bertie Formation Konservat-Lagerstätte, Ontario. *Plos One* 9 (8), e104171.
- 423 Burrow, C. J.; Trinajstić, K.; Long, J. 2012: First acanthodian from the Upper Devonian
424 (Frasnian) Gogo Formation, Western Australia. *Historical Biology* 24 (4), 349–357.
- 425 Cabrera, D. Alfredo; C., Alberto L.; Cozzuol, M. A. 2012: Tridimensional Angel Shark Jaw
426 elements (Elasmobranchii, Squatinidae) from the Miocene of Southern Argentina. *Ameghiniana*
427 49 (1), 126–131.
- 428 Caplan, M. L. & Bustin, R. M. 1999: Devonian–Carboniferous Hangenberg mass extinction
429 event, widespread organic-rich mudrock and anoxia: causes and consequences.
430 *Palaeogeography, Palaeoclimatology, Palaeoecology* 148 (4) 187–207.
- 431 Coates, M. I.; Finarelli, J. A.; Sansom, I. J.; Andreev, P. S.; Criswell, K. E.; Tietjen, K.; Rivers,
432 M. L.; La Riviere, P. J. 2018: An early chondrichthyan and the evolutionary assembly of a shark
433 body plan. *Proceedings. Biological sciences* 285, 20172418, 10 pp.
434 <http://dx.doi.org/10.1098/rspb.2017.2418>
- 435 Coates, M. I.; Gess, R. W. 2007: A new reconstruction of *Onychoselache traquairi*, comments
436 on early chondrichthyan pectoral girdles and hybodontiform phylogeny. *Palaeontology* 50 (6),
437 1421–1446.
- 438 Coates, M. I.; Gess, R. W.; Finarelli, J. A.; Criswell, K. E.; Tietjen, K. 2017: A symmoriiform
439 chondrichthyan braincase and the origin of chimaeroid fishes. *Nature* 541 (7636), 208–211.

- 440 Coates, M. I.; Sequeira, S. E. K. 2001: A new stethacanthid chondrichthyan from the lower
441 Carboniferous of Bearsden, Scotland. In *Journal of Vertebrate Paleontology* 21 (3), 438–459.
- 442 Coates, M. I.; Tietjen, Kristen; O, Aaron M.; Finarelli, J. A. 2019: High-performance suction
443 feeding in an early elasmobranch. In *Science advances* 5 (9), eaax2742.
- 444 Daegling, D. J., & Jungers, W. L. 2000: Elliptical Fourier analysis of symphyseal shape in great
445 ape mandibles. *Journal of Human Evolution*, 39(1), 107-122.
- 446 Davis, S. P.; Finarelli, J. A.; Coates, M. I. 2012: *Acanthodes* and shark-like conditions in the last
447 common ancestor of modern gnathostomes. *Nature* 486 (7402), 247–250.
- 448 Deakin, W. J., Anderson, P. S. L., den Boer, W., Smith, T. J., Hill, J., Rücklin, M., Donoghue, P.
449 C. J., Rayfield, E. J. 2022: Increasing morphological disparity and decreasing optimality for jaw
450 speed and strength during the radiation of jawed vertebrates. *Science Advances* 8, eabl3644
- 451 Dean M.N. & Summers A.P. 2006. Mineralized cartilage in the skeleton of chondrichthyan
452 fishes. *Zoology* 109, 164–168.
- 453 Dearden, R. P.; Giles, S. 2021: Diverse stem-chondrichthyan oral structures and evidence for
454 an independently acquired acanthodid dentition. *Royal Society open science* 8 (11), 210822.
- 455 DeLaurier, A. & Gerhart, J. 2018: Evolution and development of the fish jaw skeleton. *Wiley*
456 *Interdisciplinary Reviews: Developmental Biology* 8. 10.1002/wdev.337.
- 457 den Blaauwen, J.; Newman, M.; Burrow, C. 2019: A new cheiracanthid acanthodian from the
458 Middle Devonian (Givetian) Orcadian Basin of Scotland and its biostratigraphic and
459 biogeographical significance. *Scottish Journal of Geology* 55, 166-177.
- 460 Derycke, C.; Olive, S.; Groessens, E.; Goujet, D. 2015: Paleogeographical and paleoecological
461 constraints on paleozoic vertebrates (chondrichthyans and placoderms) in the Ardenne Massif
462 Shark radiations in the Famennian on both sides of the Palaeotethys. *Palaeogeography,*
463 *Palaeoclimatology, Palaeoecology* 414, 61–67
- 464 Derycke, C.; Spalletta, C.; Perri, M. C., Corradini 2008: Famennian chondrichthyan
465 microremains from Morocco and Sardinia. *Journal of Palaeontology* 82 (5), 984–995.
- 466 Dick, J. R. F. 1981: *Diplodoselache woodi* gen. et sp. nov., an early Carboniferous shark from
467 the Midland Valley of Scotland. *Earth and Environmental Science Transactions of The Royal*
468 *Society of Edinburgh* 72 (2), 99–113.
- 469 Ferrario, V. F., Sforza, C., Tartaglia, G. M., Colombo, A., & Serrao, G. 1999: Size and shape of
470 the human first permanent molar: a Fourier analysis of the occlusal and equatorial outlines.
471 *American Journal of Physical Anthropology: The Official Publication of the American Association*
472 *of Physical Anthropologists*, 108(3), 281-294.
473
- 474 Finarelli, J. A. & Coates, M. I. 2014: *Chondrenchelys problematica* (Traquair, 1888) redescribed:
475 a Lower Carboniferous, eel-like holocephalan from Scotland. *Earth and Environmental Science*
476 *Transactions of The Royal Society of Edinburgh* 105 (1), 35–59.
- 477 Frey, L., Coates, M. I., Ginter, M., Hairapetian, V., Rücklin, M., Jerjen, I., Klug, C. 2019: The
478 early elasmobranch *Phoebodus*: phylogenetic relationships, ecomorphology, and a new time-
479 scale for shark evolution. *Proceedings of the Royal Society B*, 20191336, 1-11.

- 480 Frey, L.; Coates, M. I.; Tietjen, K.; Rücklin, M.; Klug, C. 2020: A symmoriiform from the Late
481 Devonian of Morocco demonstrates a derived jaw function in ancient chondrichthyans.
482 *Communications Biology* 3 (1), 681, 1-10.
- 483 Frey, L.; Rücklin, M.; Korn, D.; Klug, C. 2018: Late Devonian and Early Carboniferous alpha
484 diversity, ecospace occupation, vertebrate assemblages and bio-events of southeastern
485 Morocco. *Palaeogeography Palaeoclimatology Palaeoecology* 496, 1–17.
- 486 Galili, T.; Benjamini, Y.; Simpson, G.; Jefferis, G.; Gallotta, M.; Renaudie, J.; Hennig, C. 2019:
487 Dendextend: Extending 'dendrogram' functionality in R. *R package version* 1.12. 0.
- 488 Giles, S.; Friedman, M.; Brazeau, M. D. 2015: Osteichthyan-like cranial conditions in an Early
489 Devonian stem gnathostome. *Nature* 520 (7545), 82–85.
- 490 Ginter, M.; Hairapetian, V.; Klug, C. 2002: Famennian chondrichthyans from the shelves of
491 North Gondwana. *Acta geologica Polonica* 52 (2), 169–215.
- 492 Ginter, M. & Maisey, J. G. (2007): The braincase and jaws of *Cladodus* from the Lower
493 Carboniferous of Scotland. In *Palaeontology* 50 (2), 305–322. DOI: 10.1111/j.1475-
494 4983.2006.00633.x.
- 495 Hanke, G. F.; Davis, S. P.; Wilson, M. V. H. 2001: New Species of the Acanthodian Genus
496 *Tetanopsyrus* from Northern Canada, and Comments on Related Taxa. *Journal of Vertebrate*
497 *Paleontology* 21 (4), 740–753.
- 498 Hanke, G. F.; Wilson, M. V. H. 2006: Anatomy of the early Devonian acanthodian
499 *Brochoadmones milesi* based on nearly complete body fossils, with comments on the evolution
500 and development of paired fins. *Journal of Vertebrate Paleontology* 26 (3), 526–537.
- 501 Harris, J. E. 1938: The neurocranium and jaws of *Cladosepache*. *Scientific publications of the*
502 *cleveland museum of natural history* 1, 1-12.
- 503 Herbert, A. M. & Motta, P. J. 2018: Biomechanics of the jaw of the durophagous bonnethead
504 shark. *Zoology* 129, 54-58.
- 505 Hill, J. J.; Puttick, M. N.; Stubbs, T. L.; Rayfield, E. J.; D., Philip C. J. 2018: Evolution of jaw
506 disparity in fishes. *Palaeontology* 61 (6), 847–854.
- 507 Hodnett, J. P. M.; Grogan, E.; Lund, R.; Lucas, S. G.; Elliott, D. 2021: Ctenacanthiform sharks
508 from the Late Pennsylvanian (Missourian) Tinajas member of the Atrasado formation, central
509 New Mexico: *New Mexico Museum of Natural History and Science Bulletin* 84, 391-424.
- 510 Johanson, Zerina; Underwood, Charlie; Richter, Martha (Eds.)- 2018: Evolution and
511 Development of Fishes. *Cambridge University Press*.
- 512 Kaesler, R. L., & Waters, J. A., 1972: Fourier analysis of the ostracode margin. *Geological*
513 *Society of America Bulletin*, 83(4), 1169-1178.
- 514 Kaiser, S. I.; Aretz, M.; Becker, R. T. 2015: The global Hangenberg Crisis (Devonian–
515 Carboniferous transition): review of a first-order mass extinction. *Geological Society, London,*
516 *Special Publications* 423 (1), 387–437.
- 517 Kaiser, S. I.; Becker, R. T.; Steuber, T.; Aboussalam, S. Z. 2011: Climate-controlled mass
518 extinctions, facies, and sea-level changes around the Devonian–Carboniferous boundary in the

- 519 eastern Anti-Atlas (SE Morocco). *Palaeogeography Palaeoclimatology Palaeoecology* 310 (3-4),
520 340–364.
- 521 Kemp, N. E. & Westrin, S. K. 1979: Ultrastructure of calcified cartilage in the endoskeletal
522 tesseræ of sharks. *Journal of morphology* 160 (1), 75–109.
- 523 Klug, C.; Frey, L.; Korn, D.; Jattiot, R.; Rücklin, M. 2016: The oldest Gondwanan cephalopod
524 mandibles (Hangenberg Black Shale, Late Devonian) and the mid-Palaeozoic rise of jaws.
525 *Palaeontology* 59 (5), 611–629.
- 526 Klug, C.; Lagnaoui, A.; Jobbins, M.; Bel Haouz, W.; Najih., A. 2021: The swimming trace
527 *Undichna* from the latest Devonian Hangenberg Sandstone equivalent of Morocco. *Swiss*
528 *Journal of Palaeontology* 140 (1), 19.
- 529 Klug, S. & Kriwet, J. 2008: A new basal galeomorph shark (Synchodontiformes, Neoselachii)
530 from the Early Jurassic of Europe. *Naturwissenschaften* 95 (5), 443–448.
- 531 Lane, J. A. & Maisey, J. G. 2012: The visceral skeleton and jaw suspension in the durophagous
532 hybodontid shark *Tribodus limae* from the Lower Cretaceous of Brazil. *Journal of Palaeontology*
533 86 (5), 886–905.
- 534 Long, J. A.; Burrow, C. J.; Ginter, M.; Maisey, J. G.; Trinajstić, K. M.; Coates, M. I.; Young, G.
535 C.; Senden, T. J. 2015: First shark from the Late Devonian (Frasnian) Gogo Formation, Western
536 Australia sheds new light on the development of tessellated calcified cartilage. *Plos one* 10 (5),
537 e0126066.
- 538 Luccisano, V.; Pradel, A.; Amiot, R.; Gand, G.; Steyer, J. S.; Cuny, G. 2021: A new *Triodus*
539 shark species (Xenacanthidae, Xenacanthiformes) from the lowermost Permian of France and
540 its paleobiogeographic implications. *Journal of vertebrate Palaeontology* 41 (2), 1-18. DOI:
541 10.1080/02724634.2021.1926470
- 542 Maisey, J. G. 1985: Cranial morphology of the fossil elasmobranch *Synechodus dubrisiensis*.
543 *American Museum novitates* no. 2804: New York, N.Y.: American Museum of Natural History.
- 544 Maisey, J. G. 2013: The diversity of tessellated calcification in modern and extinct
545 chondrichthyans. *Revue de Paléobiologie* 32 (2), 355–371.
- 546 Maisey, J. G., Denton, J. S. S., Burrow, C., Pradel, A. 2020: Architectural and ultrastructural
547 features of tessellated calcified cartilage in modern and extinct chondrichthyan fishes. *Journal of*
548 *fish biology* 98 (4), 919–941.
- 549 Maisey, J. G., Janvier, P., Pradel, A., Denton, J. S. S.; Bronson, A.; Miller, R.; Burrow, C. J.
550 2018: *Doliodus* and pucapampellids: Contrasting perspectives on stem chondrichthyan
551 morphology. In Johanson, Z., Underwood, C., Richter, M. (Eds.): Evolution and Development of
552 Fishes. *Cambridge University Press*, 87–109.
- 553 Marynowski L., Zatoń, M., Rakociński, M., Filipiak, P., Kurkiewicz, S., Pearce, T. J. 2012:
554 Deciphering the upper Famennian Hangenberg Black Shale depositional
555 environments based on multi-proxy record. *Palaeogeography, Palaeoclimatology,*
556 *Palaeoecology* 346-347, 66-86.
- 557 McGhee, G.R., 1996: The Late Devonian Mass Extinction: The Frasnian/Famennian Crisis.
558 *Columbia University Press, New York.*

- 559 McGhee, G.R., Sheehan, P.M., Bottjer, D.J., Droser, M.L., 2012: Ecological ranking of
560 Phanerozoic biodiversity crises: the Serpukhovian (Early Carboniferous) crisis had a greater
561 ecological impact than the end-Ordovician. *Geology* 40, 147–150.
- 562 McGhee, G. R., Clapham, M. E., Sheehan, P. M., Bottjer, D. J., Droser, M. L., 2013. A new
563 ecological-severity ranking of major Phanerozoic biodiversity crises. *Palaeogeography,*
564 *Palaeoclimatology, Palaeoecology* 370, 260–270.
- 565 Miles, R. S. 1970: Remarks on the vertebral column and caudalfin of acanthodian fishes.
566 *Lethaia* 3, 343–362.
567
- 568 Miles, R. S. 1973: Articulated acanthodian fishes from the Old Red Sandstone of England, with
569 a review of the structure and evolution of the acanthodian shoulder-girdle. *Bulletin of the British*
570 *Museum (Natural History). Geology* 24, 111–213.
571
- 572 Motta, P. J., Huber, D. R. 2012: Prey capture behavior and feeding mechanics of
573 elasmobranchs. In: Carrier, J. C., Musick, J. A., Heithaus, M. R. (Eds.), *Biology of Sharks*
574 *and Their Relatives. CRC Press, Boca Raton, FL* pp. 153–209.
- 575 Pradel, A.; Maisey, J. G.; Tafforeau, P.; Mapes, R. H.; Mallatt, J. 2014: A Palaeozoic shark with
576 osteichthyan-like branchial arches. *Nature* 509 (7502), 608–611.
- 577 Qiao, T.; King, B.; Long, J. A.; Ahlberg, P. E.; Zhu, M. 2016: Early Gnathostome Phylogeny
578 Revisited: Multiple Method Consensus. *Plos one* 11 (9), e0163157.
- 579 R Development Core Team. 2020: R: A Language and Environment for Statistical Computing. *R*
580 *Foundation for Statistical Computing, Vienna, Austria*, pp.
- 581 Revell, L. J. 2012: Phytools: An R package for phylogenetic comparative biology (and other
582 things). *Methods in ecology and evolution* (2), 217-223.
- 583 Rieppel, O. 1981: The hybodontiform sharks from the Middle Triassic of Monte San Giorgio,
584 Switzerland. *Neues Jahrbuch für Geologie und Paläontologie* 161 (3), 324 - 353.
- 585 Rohlf, F. J. 2015: The tps series of software. *Hystrix, the Italian Journal of Mammalogy* 26:9–12.
- 586 Romano, C. & Brinkmann, W. 2010: A new specimen of the hybodont shark *Palaeobates polaris*
587 with three-dimensionally preserved Meckel's cartilage from the Smithian (Early Triassic) of
588 Spitsbergen. *Journal of Vertebrate Paleontology* 30 (6), 1673–1683.
- 589 Rücklin, M.; King, B.; Cunningham, J. A.; Johanson, Z.; Marone, F.; Donoghue, P. C. J. 2021:
590 Acanthodian dental development and the origin of gnathostome dentitions. *Nature Ecology and*
591 *Evolution* 5 (7), 919–926.
- 592 Sallan, L. C. & Coates, M. I. 2010: End-Devonian extinction and a bottleneck in the early
593 evolution of modern jawed vertebrates. *Proceedings of the National Academy of Sciences of the*
594 *United States of America* 107 (22), 10131–10135.
- 595 Schmidt, H. 1924: Zwei Cephalopodenfaunen an der Devon-Carbongrenze im Sauerland.
596 *Jahrbuch der Preußischen Geologischen Landesanstalt* 44 (for 1923), 98–171.
- 597 Schultze, H. P.; Zidek, N. J. 1982: Ein primitiver acanthodier (pisces) aus dem Unterdevon
598 Lettlands. *Paläontologische Zeitschrift* 56 (1-2), 95–105.
- 599 Seidel R, Blumer M, Chaumel J, Amini S, Dean M.N. 2020. Endoskeletal mineralization in
600 chimaera and a comparative guide to tessellated cartilage in chondrichthyan fishes (sharks,
601 rays and chimaera). *Journal of the Royal Society Interface*. 17 (171), 20200474.

- 602 Seidel, R.; Jayasankar, A. K.; Dean, M. N. 2021: The multiscale architecture of tessellated
603 cartilage and its relation to function. *Journal of fish biology* 98 (4), 942–955.
- 604 Seidel, R.; Lyons, K.; Blumer, M.; Zaslansky, P.; Fratzl, P.; Weaver, J. C.; Dean, M. N. 2016:
605 Ultrastructural and developmental features of the tessellated endoskeleton of elasmobranchs
606 (sharks and rays). *Journal of anatomy* 229 (5), 681–702.
- 607 Wilga, C. D. & Motta, P. J. 1998: Conservation and variation in the feeding mechanism of the
608 spiny dogfish *squalus acanthias*. *The Journal of experimental biology* 201 (9), 1345–1358.
- 609 Younker, J. L., & Ehrlich, R. 1977: Fourier biometrics: harmonic amplitudes as multivariate
610 shape descriptors. *Systematic Biology*, 26(3), 336-342.
- 611 Zangerl, R.; Case, G. R. 1976: *Cobelodus aculeatus* (Cope) an anacanthous shark from
612 Pennsylvanian Black Shales of North America. *Palaeontographica, Sonder Abdruck* 154, 107–
613 157.
- 614 Zhang, M., Becker, R. T., Ma, X., Zhang, Y., Zong, P. 2019: Hangenberg Black Shale with
615 cymaclymeniid ammonoids in the terminal Devonian of South China. *Palaeobiodiversity and*
616 *Palaeoenvironments* 99: 129-142.
- 617
- 618 Zhu, M.; Yu, X.; Ahlberg, P. E.; Choo, B.; Lu, J.; Qiao, T. et al. 2013: A Silurian placoderm with
619 osteichthyan-like marginal jaw bones. *Nature* 502 (7470), 188–193.

Figure 1

Meckel's cartilage outlines and close ups

Meckel's cartilage of a ctenacanth chondrichthyan from the Hangenberg black shale, Madene El Mrakib; PIMUZ A/I 5139. A, lateral view; B₁, traced outline and ventral ridge; B₂, counterpart with outline; C, Close up of the anterior area; D, close up of the posterior area; E_{1,2}, Close-up photos of the cartilage showing the polygonal pattern. Abbreviations: sym - symphysis, ma - muscle attachment area, vr - ventral ridge, re.fl - retroarticular flange. Scale bar for A, B_{1,2} equals 5 mm. Scale bar for C, D, E_{1,2} equals 1 mm. Arrow indicates Anterior (A) and Posterior (P).

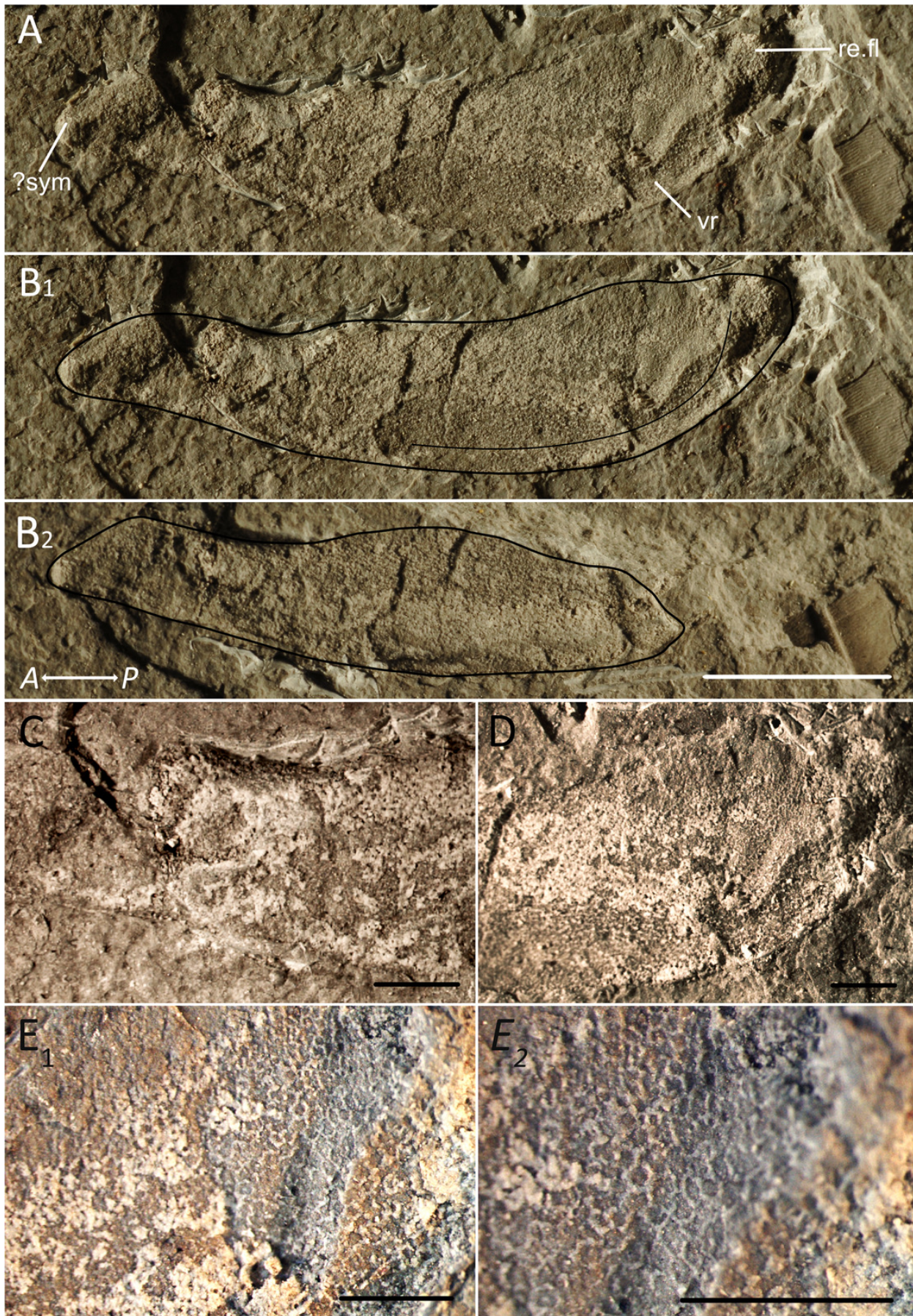


Figure 2

PCA and morphospace with all sampled lower jaws

Principal Component Analysis of some fossil and modern chondrichthyan lower jaws. Orange colours: acanthodians; purple colours: holocephalan; blue colours: elasmobranchs. The new lower jaw from the Hangenberg black shale is represented by a black dot and grey colours represent lower jaws of unknown class and order. A jaw morphospace is represented in the background showing the shape variation. The new Hangenberg black shale jaw plots close to jaws of acanthodians as well as elasmobranchs. Lv: *Latviacanthus ventispilsensis*, Is: *Ischnacanthus* sp., Po: *Palidiplospinax occultidens*, Dh: *Dracopristis hoffmanorum*, Ct: *Ctenacanthus* sp. Hd: *Heslerodus divergens*.

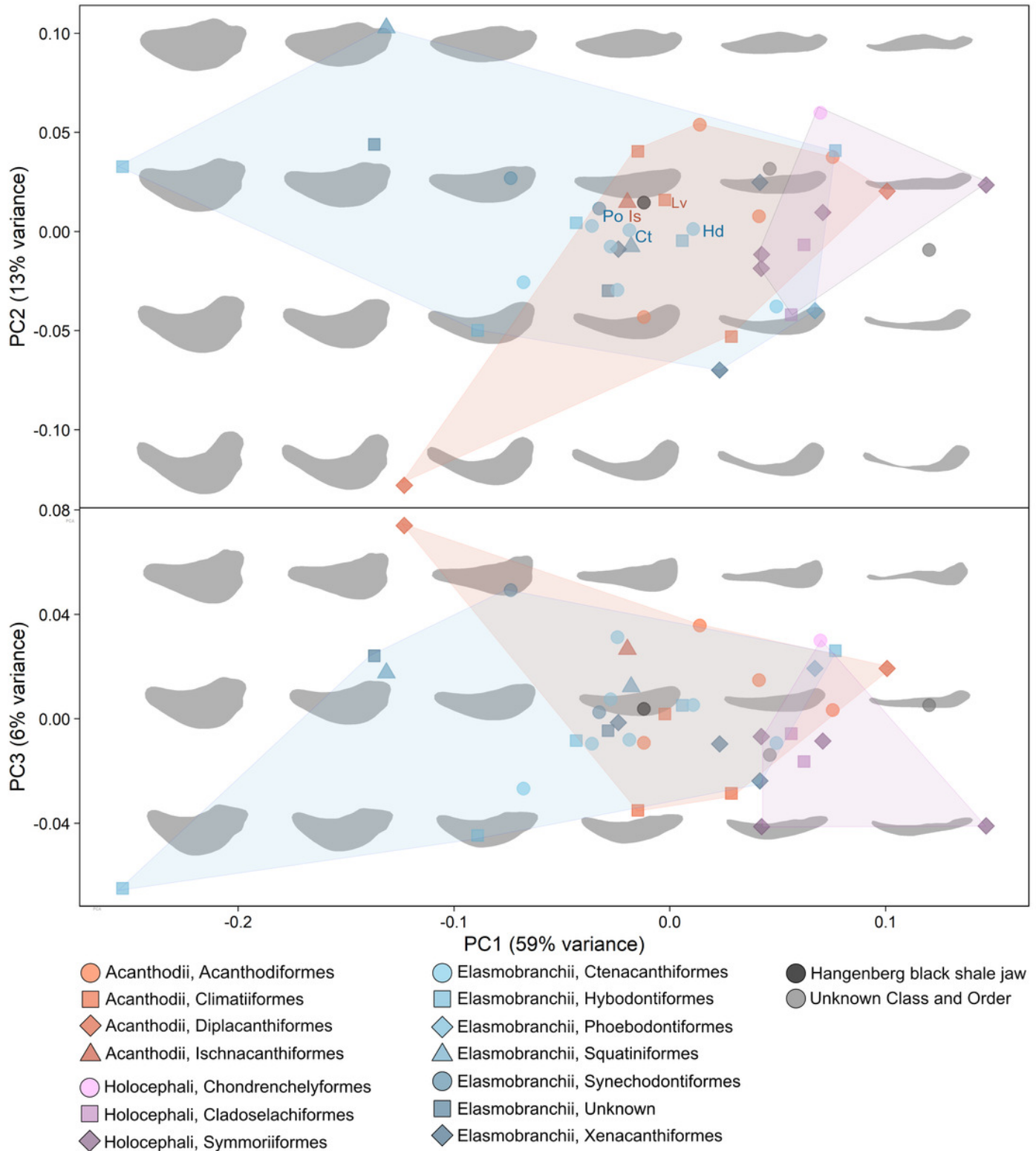


Figure 3

Dendrogram showing morphological distances of the sampled lower jaws

Dendrogram showing morphological distances regarding the first principal components from the PCA. Orange colours: acanthodians; purple colours: holocephalan; blue colours: elasmobranchs. The elasmobranchs plot mainly on the top, while holocephalan jaws plot mainly at the bottom. Acanthodian jaws are scattered over the whole dendrogram. The lower jaw from the Hangenberg black shale is closest to some acanthodian jaws such as that of *Ischnacanthus* sp.

Morphological distance

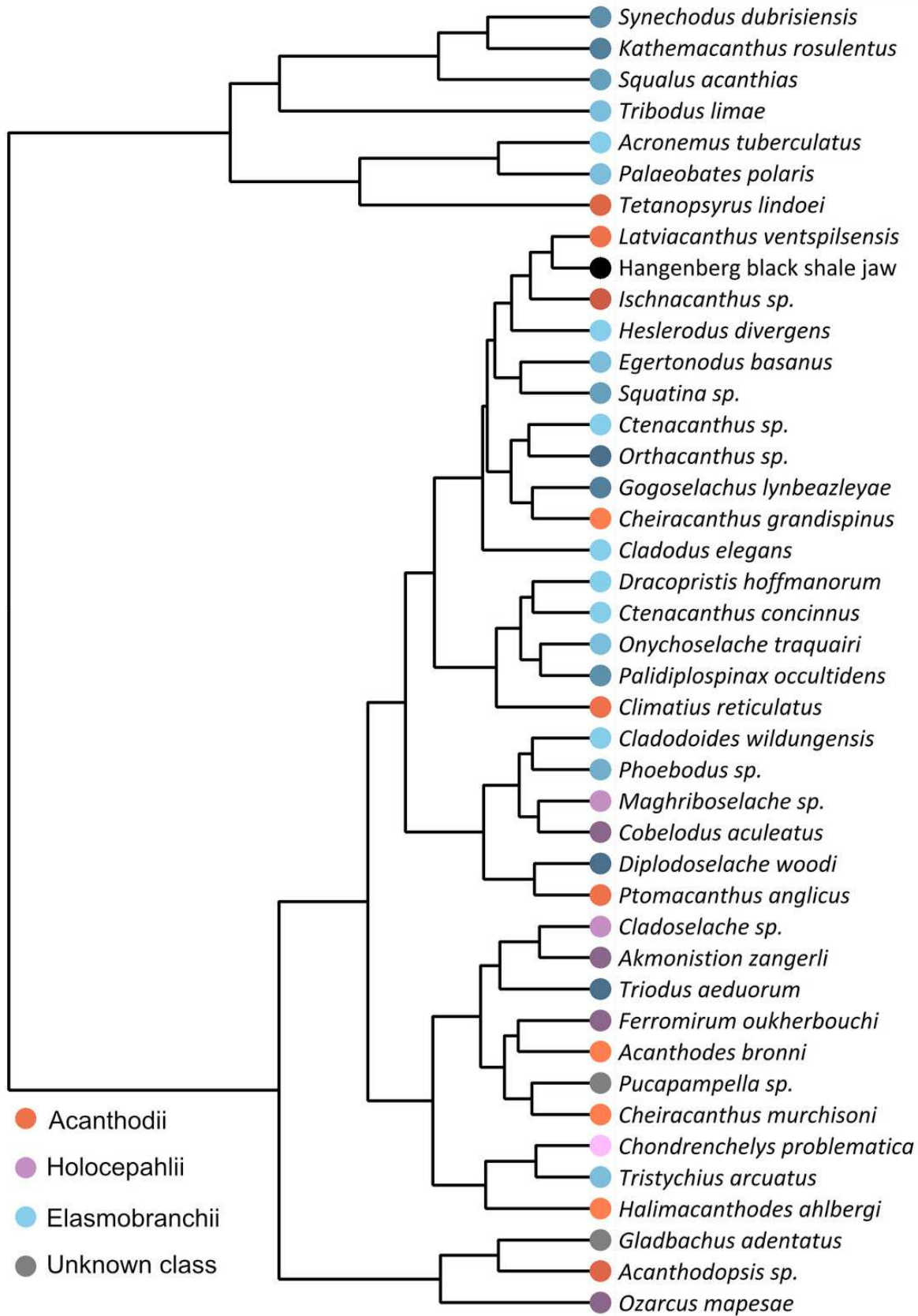


Figure 4

Phylogenetic signal metrics and tests of significance

Phylogenetic signal metrics and tests of significance performed in 1000 trees accounting for phylogenetic and stratigraphic uncertainty.

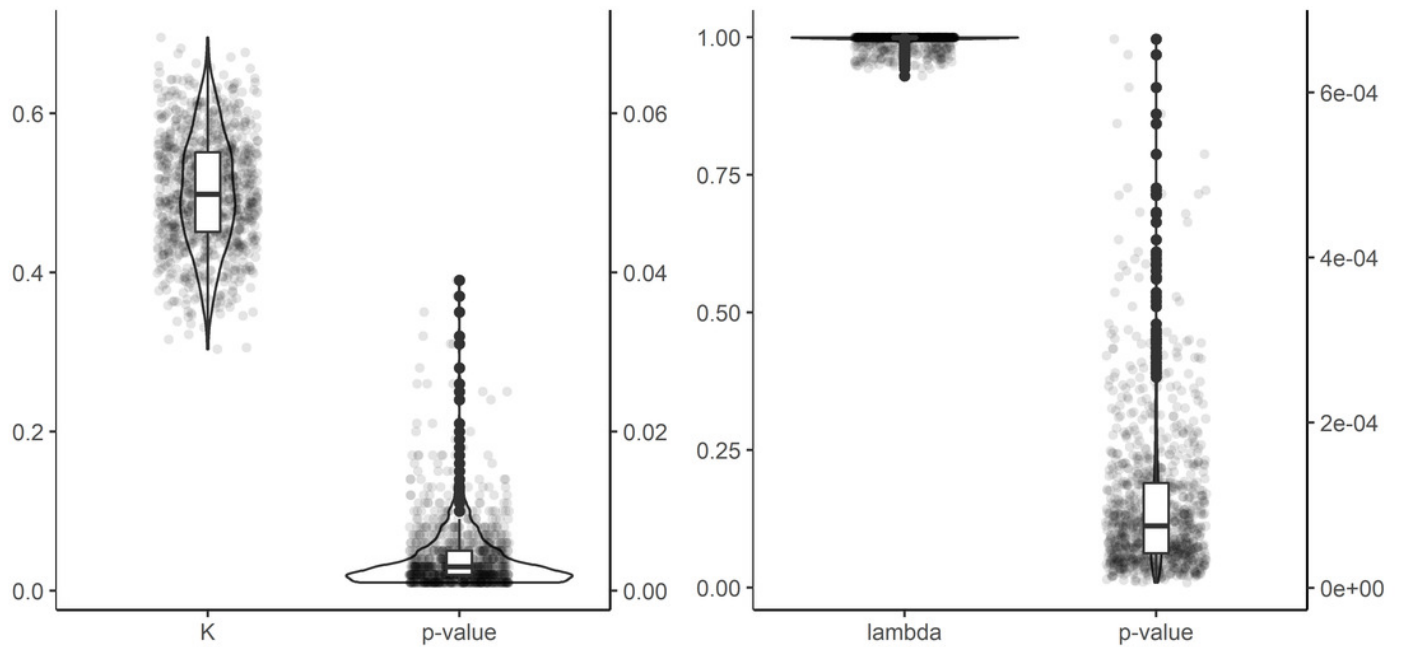


Figure 5

Mantel test results

Results of the Mantel test analysis performed in 1000 trees accounting for phylogenetic and stratigraphic uncertainty. R statistic values close to 1 or -1 support strong correlation, while values close to 0 support weak correlation

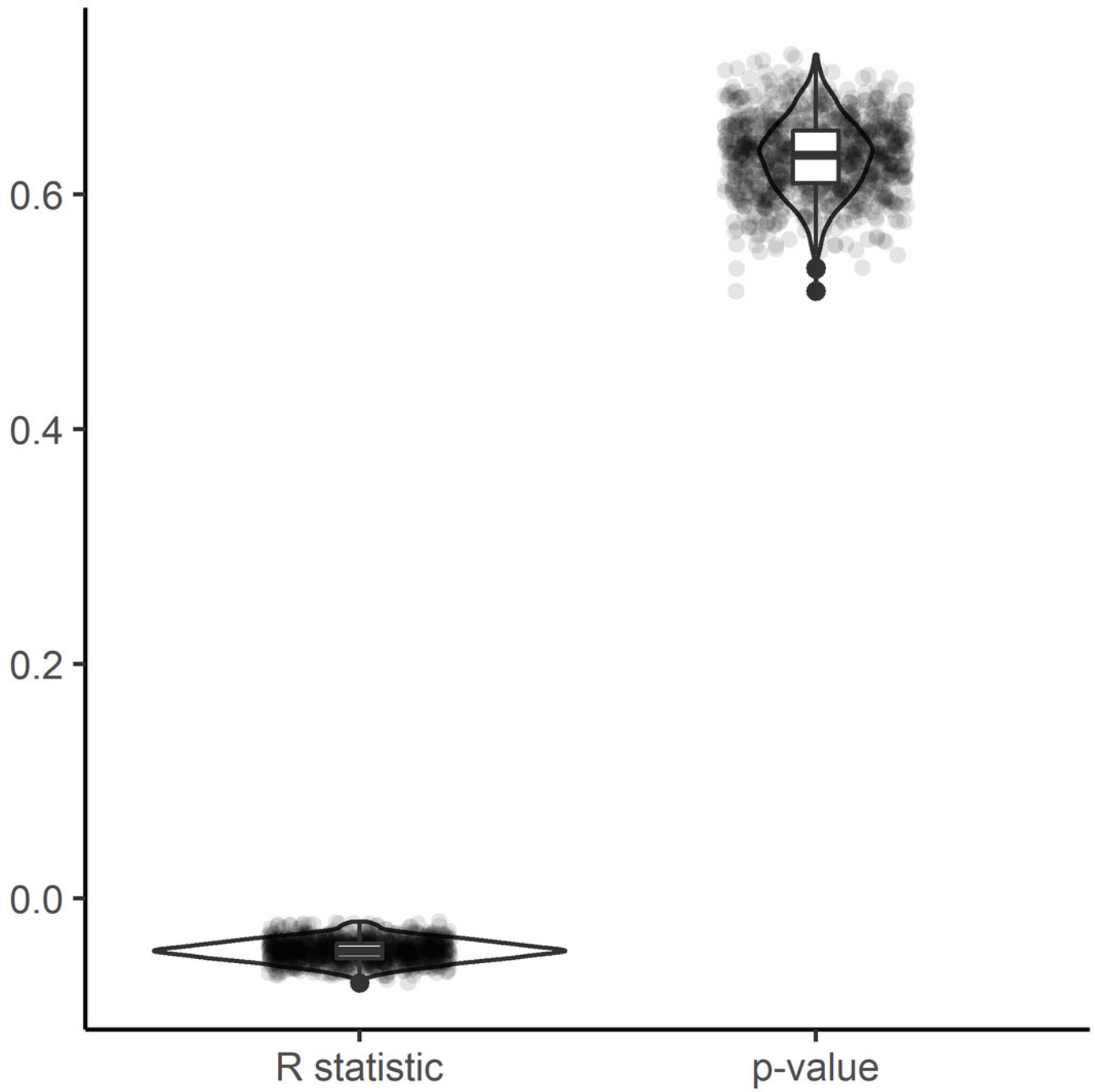
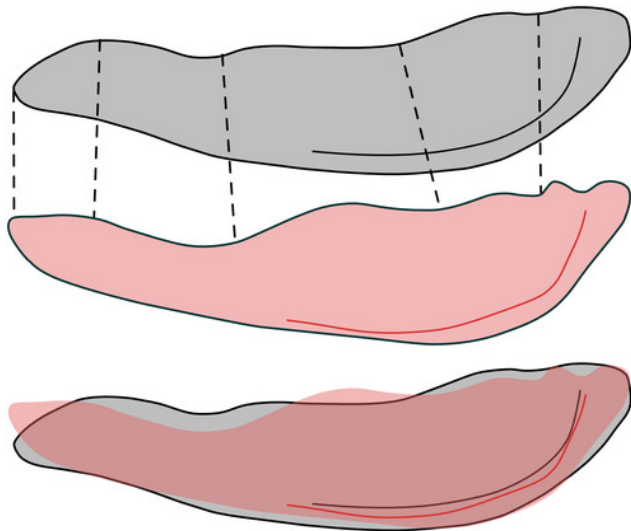


Figure 6

visual jaw shape comparison

Direct comparison of the new HBS Meckel's cartilage (grey, top) with the two most similar jaw shapes of two different groups (pink, middle) and an overlay of both (pink and grey, bottom). A: the elasmobranch *Heslerodus divergens*. B: the acanthodian *Ischnacanthus* sp. Different characteristic points, that were not captured by the PCA directly, as well as the ventral ridge are compared and both shapes are shown in overlap with the HBS Meckel's cartilage.

A: HBS Meckel's cartilage and *Heslerodus divergens*



B: HBS Meckel's cartilage and *Ischnacanthus* sp.

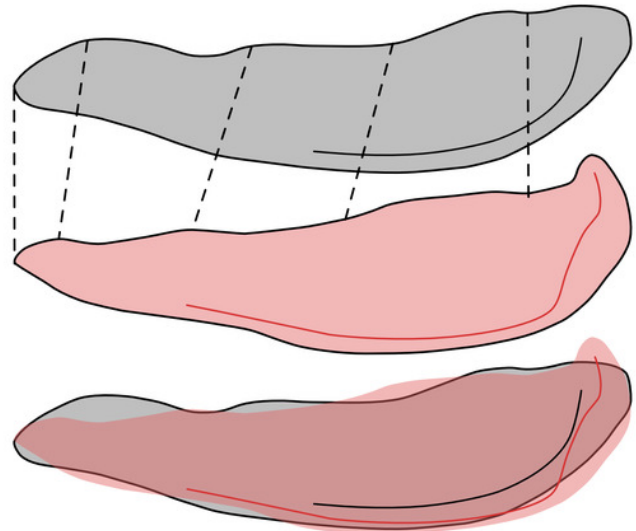


Figure 7

All sampled outlines in a phylogenetic tree showing the possible position of the new Meckel's cartilage

Simplified chondrichthyan phylogeny modified after Klug et al. (in prep.). The lower jaw from the Hangenberg black shale is figured together with the taxa used in the Fourier Analysis. The shapes of the lower jaws were redrawn from the literature (App. 1). The new HBS jaw is suggested to be of ctenacanthiform origin regarding the analyses and comparison of characters.

